Two-photon-excited luminescence and defect formation in SiO_2 nanoparticles induced by 6.4-eV ArF laser light

Yuri D. Glinka*
Institute of Atomic and Molecular Sciences, Academia Sinica, P.O. Box 23-166, Taipei 106, Taiwan and Institute of Surface Chemistry of the National Academy of Sciences of Ukraine, Prospekt Nauki 31, Kiev 252650, Ukraine

Sheng-Hsien Lin and Yit-Tsong Chen
Institute of Atomic and Molecular Sciences, Academia Sinica, P.O. Box 23-166, Taipei 106, Taiwan and Department of Chemistry, National Taiwan University, Taipei 106, Taiwan
(Received 3 January 2000; revised manuscript received 24 March 2000)

The photoluminescence (PL) from 7- and 15-nm silica (SiO_2) nanoparticles induced both by ArF laser light [$\lambda_{exc}=193$ nm (6.4 eV), $\tau_L=15$ ns] and by Nd:YAG (yttrium-aluminum-garnet) laser light [$\lambda_{exc}=266$ nm (4.66 eV), $\tau_L=8$ ns] was studied. The laser light intensity dependencies of the PL yields reveal the two-photon (TP) process of the PL excitation in the case of ArF laser light. The PL results from the radiative relaxation of self-trapped excitons (STE- the blue band), also from the surface hydrogen-related species (the green band), and the bulk nonbridging oxygen hole centers (NBOHC's- the red band) excited by a radiationless relaxation of TP-produced free excitons (FE's). The main point is focused on the effect of the nanoparticle surface condition on the FE dynamics. The dynamics includes either an elastic scattering or quenching by the nanoparticle boundary, the laser heating of FE's up to energies in excess of the STE barrier, the FE energy transfer to the surface and bulk NBOHC's and hydrogen-related centers, the saturation of the FE density, and the biexciton process in the formation of Frenkel defects with their subsequent transformation into NBOHC's.

I. INTRODUCTION

Silicon dioxide (SiO_2) is a typical wide band-gap insulator (the band-gap of bulk silica $E_g \cong 11$ eV Ref. 1), therefore the bulk SiO_2-based materials are characterized by high transparency in the ultraviolet spectral range, resulting in many important technological applications. The properties of these materials have been extensively studied for an appreciable length of time and quite well established.[1–29] On the other hand, modern nanoscale technology requires the production of nanometer-sized SiO_2 films and layers, which are of frequent use in silicon-based electronic devices for passivation and electrical insulation. Since the properties of silica-based nanoscale materials are assumed to be different from those of the bulk specimens, a great body of investigations was recently devoted to the study of nanoscale SiO_2 solids.[30–39] From the physical point of view, there is an interest to compare the properties of bulk and nanometer-sized silicas, especially those that are related to the carrier and exciton transport. The last process is assumed to be responsible for the defect formation in silicon dioxide and affects its optical and electrical properties. Silica nanoparticles with diameters in the range of several tens of nanometers or less are excellent candidates to reach the mentioned goal. Note also that the discussed spectroscopic properties of nanoscale SiO_2-based materials are closely related to the problem of $\equiv$Si-H and $\equiv$Si-O• species in silicon-hydrogen alloy films and porous silicon.[40–43] The photoluminescence (PL) from porous silicon is very promising for quantum electronics, but the origin of this emission has not yet been completely clarified. Since the mentioned species are abundant in the silica-based nanoscale materials, the study of silica nanoparticles is also of profound importance for the silicon-based electronic technology.

Many spectroscopic studies were devoted on structural defects in crystalline and glassy SiO_2 generated by using excimer lasers,[2,4–6,8–10,12,18] electron beams,[1,10,25,29,36,37] neutrons,[1,10,16,24] ion implantation,[32] or an ionizing radiation.[1,10,16,24,28] Tsai and Griscom proposed an excitonic mechanism for defect formation in SiO_2.[9] Because an intermediate case between two main types of excitons (the Frenkel and Mott-Wannier excitons) occurs in wide band-gap materials, including SiO_2, the free excitons (FE's) and the self-trapped excitons (STE's) coexist in these materials.[1,44] It is known that the self-trapping of FE's is accompanied by a strong distortion of the SiO_2 lattice, which leads to a large Stokes shift of the STE PL (STEPL) band. As a result from this the intrinsic recombination appears as an emission band peaked at $\sim$2.75 eV with a full width at half maximum of $\sim$0.7 eV and lifetime $\tau \sim 1$ ms.[3] This emission is attributed to a triplet-to-singlet transition in STE and can be induced by ultraviolet light,[3] energetic electrons,[29] x rays,[1] or multiphoton (MP) excitation.[11,31] Totally, there are several channels for the FE energy relaxation, including the mentioned self-trapping followed by STEPL, the FE energy transfer to impurities and structural defects with the subsequent excitation of their intrinsic emission, and the radiationless decay and/or defect formation.[1] It is well known that the self-trapping process results from a localization of FE's in lattice, which requires a reduction in the FE energy.[44] As this takes place, it

is predicted that there exists a self-trapping barrier for FE's in order to reach self-trapped states, which can be passed either by tunneling or by activation.[44] According to this statement, it is reasonable to expect that the FE's should be heated up to an energy exceeding the activation barrier before being self-trapped. The resulting energy reduction due to the self-trapping gives rise to the STE states inside the energy gap. For instance, the STE can be generated directly in glassy SiO_2 by using photons with energy in the range of 8.3–9.6 eV, that is, smaller than the energy gap.[3,31]

Griscom proposed a model of STE in SiO_2 based on an assumption that the electronic component of the STE is an E' center (oxygen vacancy) and the hole one is a peroxy linkage (≡Si-O-O-Si≡).[29] As a radiationless channel in the STE decay, the formation of Frenkel defects has been suggested.[2,9] Arai and co-authors[2] used nanosecond-pulsed 6.4-eV ArF laser light to observe a two-photon (TP) process of the defect formation in silica glasses. Later Tsai and Griscom [9] using the same TP excitation evidenced that peroxy radicals (≡Si-O-O•) and O_2 molecules (Frenkel defects) are created through the biexciton process of the STE decay. Shluger and Stefanovich[7] on the basis of a theoretical calculation proposed the formation of peroxy linkages and oxygen vacancies as a consequence of the STE relaxation. Skuja and Guttler[15] and Hosono, Kawazoe, and Matsunami[27] finally confirmed the existence of Frenkel defects from an infrared PL study of singlet O_2 in SiO_2 materials. Also, since a peroxy linkage is considered to be a precursor for the nonbridging oxygen hole centers (NBOHC's):[12]

$$\equiv\text{Si-O-O-Si}\equiv \rightarrow \equiv\text{Si-O}\bullet\bullet\text{O-Si}\equiv, \qquad (1)$$

this process can be involved in the STE decay as well. Hence, the FE relaxation in SiO_2 materials is expected to be very complicated and includes both radiative and radiationless steps.

According to this statement, it would be very interesting to probe the FE dynamics in silica-based nanoscale materials. To our knowledge, such a consideration has not been carried out before. In the current paper, we present experimental data devoted to the study of TP-excited PL from amorphous silica nanoparticles induced by 6.4-eV ArF laser light ($\lambda_{exc}=193$ nm). The PL spectra measured with the Nd:YAG (yttrium-aluminum-garnet) laser excitation ($\lambda_{exc}=266$ nm) were used as supporting data. Particular emphasis has been placed on the effect of the nanoparticle surface condition on the dynamics of TP-produced FE's. The surface conditions of silica nanoparticles were examined within Fourier-transform infrared (FTIR) measurements. It has been proposed that the FE dynamics includes either an elastic scattering or quenching by the nanoparticle boundary, the FE laser heating process followed by self-trapping, the FE energy transfer to surface and bulk defects, and the saturation of the FE density and the biexciton process in the formation of Frenkel defects with their subsequent transformation into NBOHC's.

II. EXPERIMENTAL SECTION

Two kinds of silica powders (Aerosil, Degussa) with the nominal particle size of 7 and 15 nm (diameter) were studied. The powders have been pressed into pellets and then dehydrated at different temperatures $T_{ht}=300$ (the initial sample), 873, and 1173 K for 2 h in air. The PL measurements were performed in a vacuum chamber at room temperature using both an ArF pulsed laser [$\lambda_{exc}=193$ nm(20 ns); Lumonics, EX-742] with a repetition rate of 10 Hz and a Nd:YAG pulsed laser [$\lambda_{exc}=266$ nm(8 ns); Spectra Physics, GCR-190] with a repetition rate of 30 Hz as sources of excitation. The laser beams have been focused by a 30-cm lens into a 0.03-cm^2 spot. Any sample damages were not observed during laser light irradiation in the applied range of intensities. The intensity of laser light could be varied by a set of quartz plates. The sample was placed on a copper holder and oriented to the laser beam by 45°. The PL was collected in a conventional 90° geometry by a 0.5-m SpectraPro-500 monochromator (Acton Research Corporation) with 1200 lines/mm grating. The monochromator spectral slit width was ~0.7 nm. The spectra were recorded by using a charge coupled device camera (Princeton Instruments, 330×1100 pixels) within an accumulation time of 2 s. The data acquisition was processed in a computer equipped with a CSMA software (Princeton Instruments). A set of color filters has been used in order to cut stray radiation from lasers and scattered laser light from samples. The intensity dependencies of the PL yields (IDPLY) were measured by using the CCD camera within an accumulation time of 10 s for each of laser light intensities. FTIR measurements were performed in a vacuum at room temperature using a Bruker IFS-113 v spectrometer with a resolution of 4 cm^{-1}.

III. RESULTS AND DISCUSSION

A. FTIR control of the nanoparticle surface condition

Because the silica nanoparticles are characterized by a large surface/volume ratio, they contain a great deal of surface structural defects (≡Si• and ≡Si-O•). These defects result from the splitting of the ≡Si-O-Si≡ regular bonds at the moment of nanoparticle formation. As this takes place, the nanoparticles are in a nonequilibrium condition with respect to the adsorption-desorption process. Hydrogen atoms normally block these defects, forming hydrogen-related species on the surface (≡Si-H and ≡Si-OH). The mentioned species are assumed to be a controlling factor in the aggregation of nanoparticles into micron-sized composites (globules) and weblike microstructures.[32,34,39] They are also the original sites for the molecule adsorption. It is known that water molecules completely reduce the adsorption activity of the silica nanoparticle surface. As a consequence, the silica nanoparticle composites come to an equilibrium condition, which corresponds to initial powders. The heat treatment in air varies the nanoparticle surface condition because of water removing. This process is usually termed as an activation of the silica nanoparticle surface.

Since our main interest here is the probe of the nanoparticle surface condition on the TP-excited PL, we have controlled the content of hydrogen-related species and adsorbed water with heat pretreatment temperature ($T_{ht}=300-1173$ K). For this purpose, FTIR spectra for the silica nanoparticle composites in the range of the stretching vibrations of ≡Si-OH and H_2O were measured. The dynamics of FTIR spectra as a function of T_{ht} is shown in Fig. 1. The spectra were deconvoluted by Gaussian profiles. Figure 2

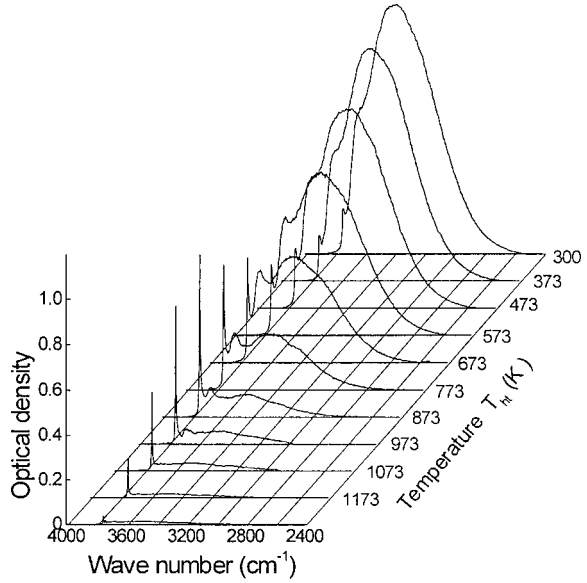

FIG. 1. The FTIR spectra of 15-nm silica particles as a function of heat pretreatment temperature (T_{ht}).

shows, as an example, the typical spectrum for the sample of 15-nm silica particles heat pretreated at $T_{ht}=673$ K and corresponding Gaussian components. The spectra are very similar to those that have been obtained for the larger sized nanoparticles.[46] According to previous data,[35,45] the absorption bands can be interpreted as follows: 3748 cm^{-1}, O-H stretching vibration in a free hydroxyl group on the surface of silica nanoparticles (≡Si-OH); 3736 cm^{-1}, O-H stretching vibration in free hydroxyls, but weakly perturbed by neighboring adsorbed water on the surface; 3660 cm^{-1}, O-H stretching vibration in hydroxyls located inside silica nanoparticles; 3490, 3250 cm^{-1}, O-H stretching vibration in two different kinds of adsorbed water molecules on the surface; and 2965 cm^{-1}, O-H stretching vibration in adsorbed water dimers. The dependencies of integrated intensities for the absorption bands related to each of the kinds of species against the heat pretreatment temperature are shown in Fig. 3. It can be easily seen that the amount of free and weakly perturbed hydroxyls increases in the same temperature range as a consequence of water removing from the surface. When T_{ht} comes to 873 K, the water is practically desorbed,

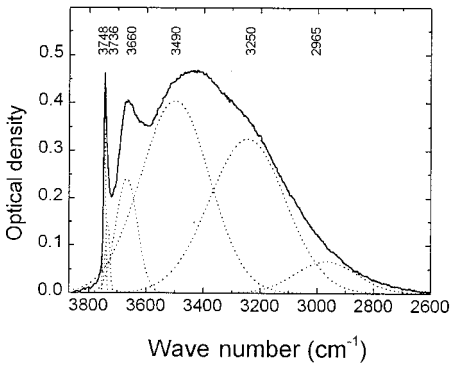

FIG. 2. An example of the FTIR spectrum deconvoluted by Gaussian profiles for 15-nm silica particles. Numbers denote the absorption peak position of the corresponding Gaussian components.

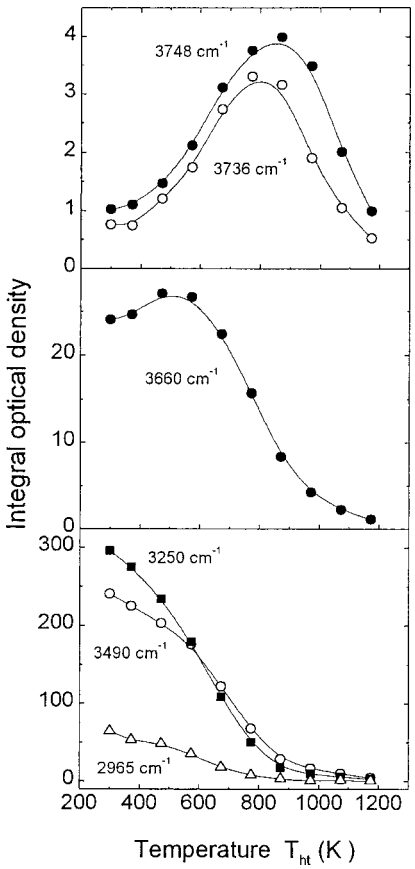

FIG. 3. The heat pretreatment temperature dependencies of the integral intensity of the FTIR bands for 15-nm silica particles. Numbers denote the position of absorption peaks.

whereas the amount of free and weakly perturbed hydroxyls reaches a maximum. After this temperature the concentration of free hydroxyls goes down, indicating the destruction process followed by the NBOHC's formation.[34,35,45]

$$2(\equiv\text{Si-OH}) \xrightarrow{T_{ht}\geqslant 873\ \text{K}} (\equiv\text{Si-O}\bullet)+(\equiv\text{Si}\bullet)+H_2O\uparrow. \quad (2)$$

$$2(\equiv\text{Si-OH}) \xrightarrow{T_{ht}\geqslant 873\ \text{K}} (\equiv\text{Si-O}\bullet\bullet\text{O-Si}\equiv)+H_2\uparrow. \quad (3)$$

Note that similar reactions are expected to occur for bulk species as well (the 3660 cm^{-1} band). However, the destruction process for bulk hydroxyls begins with smaller temperature.

Subsequently, the surface of silica nanoparticles is almost completely dehydrated at $T_{ht}=1173$ K and structure defects cover the surface. Thus, we can conclude that there exist three special heat pretreatment temperatures for silica nanoparticles: $T_{ht}=300$ K corresponds to initial powders, at which the nanoparticle surface is covered by hydrogen-related species and adsorbed water; $T_{ht}=873$ K is associated with the condition, at which adsorbed water is removed, but hydrogen-related species still cover the surface; $T_{ht}=1173$ K corresponds to the completely dehydrated surface with a great deal of structure defects on it (Fig. 4). According to this model, we have measured PL spectra from the samples prepared at three above-mentioned heat pretreatment temperatures. Of course, the surface condition variation pro-

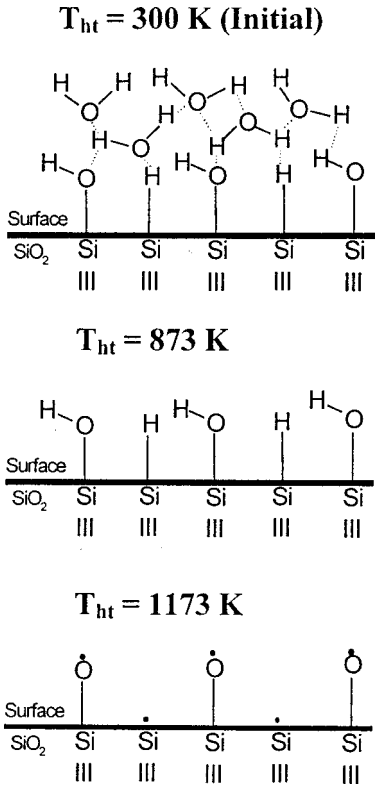

FIG. 4. The proposed model for the silica nanoparticle surface conditions following to the FTIR measurements.

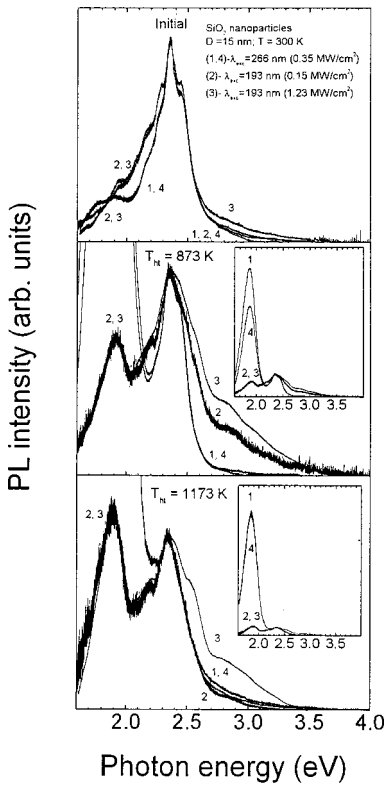

FIG. 5. A dynamics of the PL spectra for 15-nm silica particles with heat pretreatment temperature (T_{ht}). The spectra were normalized at the 2.37-eV PL band; $\lambda_{exc}=266$ nm, $I_L=0.35$ MW/cm^2 (1,4); $\lambda_{exc}=193$ nm, $I_L=0.15$ MW/cm^2 (2); $\lambda_{exc}=193$ nm, $I_L=1.23$ MW/cm^2 (3). Curves 1 and 4 correspond to the nonirradiated and preirradiated with $\lambda_{exc}=193$ nm, $I_L=1.23$ MW/cm^2 samples, respectively. Insets show the same PL spectra on a reduced scale. Curves 1 and 3 correspond to those in Ref. 39.

posed for silica nanoparticles is a simplified approximation. It has been shown experimentally that a certain part of hydroxyls is already transformed to NBOHC's at $T_{ht}=873$ K, giving rise to the corresponding PL response.[34,35,39] Also, a certain concentration of hydrogen-related centers remains to be present on the surface even at $T_{ht}=1173$ K.[39] However, as it will be shown in the next sections, the use of this approximation nevertheless allows us to understand the main specific features in the dynamics of TP-produced FE's in silica nanoparticles.

B. The PL spectra from silica nanoparticles

The PL spectra from 15- and 7-nm silica particles induced both by ArF and by Nd:YAG (see p. 2) laser light ($\lambda_{exc}=193$ or 266 nm) for the mentioned three conditions of the silica nanoparticle surface are shown in Figs. 5 and 6, respectively. Overall, one can observe three bands located in the blue, green, and red spectral ranges. The green band peaked at ~2.37 eV (523 nm) is characterized by a progression and was assigned to hydrogen-related species in our previous study.[35,39] It has been shown that the progression is caused by electron-vibrational coupling in ≡Si-H species, resulting from interaction between electronic transitions and ≡Si-H bending vibration in the ground electronic state.[39] Because the green PL band intensity did not vary within the given time of laser irradiation, it has been selected to normalize the intensity of spectra taken at different experimental conditions (Figs. 5 and 6).

The red PL band induced by 193-nm light is peaked at ~1.9 eV, whereas it is shifted towards the long wavelength side with 266-nm excitation. According to previous data, the shift results from the existence of two bands peaked at ~1.9 and ~1.79 eV (652 and 693 nm), which were assigned to bulk and surface NBOHC's, respectively.[39] Note that the red bands enhance significantly with T_{ht} in full agreement with the proposed reactions (2) and (3).[34,39] Since the photon energy of Nd:YAG laser light (266 nm, 4.66 eV) coincides very closely with the absorption peak of the NBOHC (~4.8 eV Refs. 13 and 16) comparing to ArF laser light (193 nm, 6.4 eV), both of the kinds of species located either inside nanoparticles or on their surfaces are able to emit light in the case of 266-nm excitation. However, only bulk NBOHC's can be excited by 193-nm light. This experimental fact indicates the existence of two different mechanisms in PL excitation. We propose that an ordinary one-photon direct process of the intrinsic PL excitation from NBOHC's takes place when 266-nm light is used. Meanwhile, it should be considered an indirect mechanism under 193-nm excitation. The indirect excitation is suggested to be due to the generation of TP-produced FE's in silica nanoparticles followed by the radiationless FE energy transfer to NBOHC's. As a result, the NBOHC's becomes excited and the corresponding deexcitation gives the emission. Since one can observe just a single PL band related to the bulk NBOHC's when 193-nm light is applied, the FE interaction with the surface NBOHC is expected to be without energy transfer to this center. In other words, we predict that the FE, interacting with the

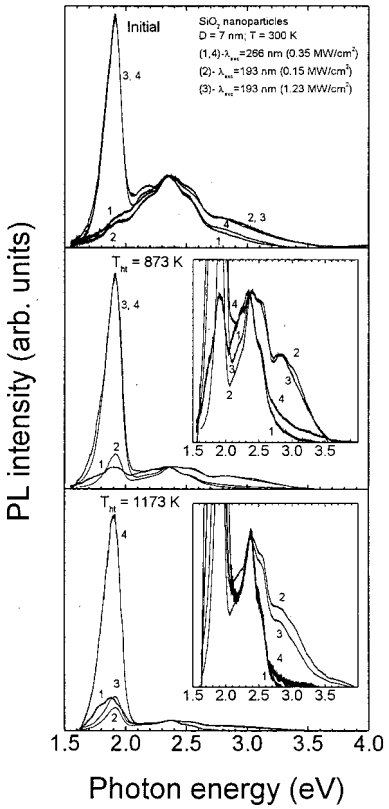

FIG. 6. A dynamics of the PL spectra for 7-nm silica particles with heat pretreatment temperature (T_{ht}). The spectra were normalized at the 2.37-eV PL band; $\lambda_{\mathrm{exc}}=266$ nm, $I_L=0.35$ MW/cm^2 (1,4); $\lambda_{\mathrm{exc}}=193$ nm, $I_L=0.15$ MW/cm^2 (2); $\lambda_{\mathrm{exc}}=193$ nm, $I_L=1.23$ MW/cm^2 (3). Curves 1 and 4 correspond to the nonirradiated and preirradiated with $\lambda_{\mathrm{exc}}=193$ nm, $I_L=1.23$ MW/cm^2 samples, respectively. Insets show the same PL spectra on an enlarged scale. Curves 1 and 2 correspond to those in Ref. 39.

surface NBOHC, suffers an elastic scattering. We will clarify this conclusion in the next section.

The blue band peaked at ~2.8 eV (443 nm) appears as a shoulder near the 2.37-eV band and can only be induced by 193-nm light (Figs. 5 and 6). This PL band is attributed to an emission resulted from a radiative relaxation of STE's. Totally, we propose that the PL spectra measured with 193-nm excitation originate from hydrogen-related species (the 2.37-eV band) and NBOHC's (the 1.9-eV band) excited by a radiationless relaxation of TP-produced FE's. Because the FE's are able to be self-trapped, one can additionally observe the 2.8-eV PL band related to STE's. It is evident that the blue band should be absent in the spectrum taken with 266-nm excitation because the total energy of two laser photons (9.32 eV) is not enough to produce FE's (10.2 eV Ref. 1), which could be self-trapped and then emit light. However, as we mentioned in the Introduction, the possibility exists to generate STE's directly in glassy SiO_2 by using photons with energy in the range of 8.3–9.6 eV.[3,31] Therefore, one can expect a direct TP process of STE generation by 266-nm laser light. Since in using such a source of excitation we did not observe the PL response related to STE's, we confirm the fact that the excitation of PL in this case does not involve any excitonic states, hence is due to the one-photon absorption process. Taking in to account these data, we have concluded that the 266-nm light intensity used in our experiments was not enough to initiate the TP absorption.

Thus, we propose two different mechanisms for PL excitation in silica nanoparticles. One of them is a direct one-photon excitation of intrinsic PL from NBOHC's and hydrogen-related centers, which occurs when 266-nm laser light is applied:

$$
\begin{aligned}
&(\equiv\mathrm{Si\text{-}O}\bullet)_b \xrightarrow{4.66\ \mathrm{eV}} (\equiv\mathrm{Si\text{-}O}\bullet)_b^*\\
&(\equiv\mathrm{Si\text{-}O}\bullet)_b^* \xrightarrow{1.9\ \mathrm{eV}} (\equiv\mathrm{Si\text{-}O}\bullet)_b\\
&(\equiv\mathrm{Si\text{-}O}\bullet)_s \xrightarrow{4.66\ \mathrm{eV}} (\equiv\mathrm{Si\text{-}O}\bullet)_s^*\\
&(\equiv\mathrm{Si\text{-}O}\bullet)_s^* \xrightarrow{1.79\ \mathrm{eV}} (\equiv\mathrm{Si\text{-}O}\bullet)_s,\\
&(\equiv\mathrm{Si\text{-}H})_s \xrightarrow{4.66\ \mathrm{eV}} (\equiv\mathrm{Si\text{-}H})_s^*\\
&(\equiv\mathrm{Si\text{-}H})_s^* \xrightarrow{2.37\ \mathrm{eV}} (\equiv\mathrm{Si\text{-}H})_s,
\end{aligned}
\tag{4}
$$

where stars denote excited states and *b* and *s* correspond to the bulk and surface species, respectively.

The second mechanism is an indirect excitation of the mentioned PL centers by radiationless relaxation of TP-produced FE's. This happens when 193-nm light is used (total energy 12.8 eV). The excitonic energy transfer to the PL centers with their subsequent excitation is responsible for PL in this case:

$$
\begin{aligned}
&(e-h)_{\mathrm{FE}}+(\equiv\mathrm{Si\text{-}O}\bullet)_b\rightarrow(\equiv\mathrm{Si\text{-}O}\bullet)_b^*,\\
&(\equiv\mathrm{Si\text{-}O}\bullet)_b^* \xrightarrow{1.9\ \mathrm{eV}} (\equiv\mathrm{Si\text{-}O}\bullet)_b,\\
&(e-h)_{\mathrm{FE}}+(\equiv\mathrm{Si\text{-}H})_s\rightarrow(\equiv\mathrm{Si\text{-}H})_s^*,\\
&(\equiv\mathrm{Si\text{-}H})_s^* \xrightarrow{2.37\ \mathrm{eV}} (\equiv\mathrm{Si\text{-}H})_s.
\end{aligned}
\tag{5}
$$

Because the FE relaxation on the surface NBOHC is suggested to occur without energy transfer (an elastic scattering), the PL response from the surface NBOHC's is absent. Additionally, the self-trapping of FE's followed by radiative relaxation gives the STEPL:

$$
\begin{aligned}
&(e-h)_{\mathrm{FE}}\rightarrow(e-h)_{\mathrm{STE}},\\
&(e-h)_{\mathrm{STE}} \xrightarrow{2.8\ \mathrm{eV}} (\equiv\mathrm{Si\text{-}O\text{-}Si}\equiv)_b.
\end{aligned}
\tag{6}
$$

As discussed in the Introduction, the relaxation of FE's generated in silica nanoparticles by 193-nm light can lead to the defect production (NBOHC's). Therefore, we used 266-nm light to detect intrinsic defects, which could be produced by 193-nm light irradiation. For this purpose, we measured four spectra for each sample: (1) the spectrum mea-

sured with 266-nm light, (2) the spectrum measured with weak 193-nm light, (3) the spectrum measured with strong 193-nm light, and (4) the spectrum from the sample preirradiated with strong 193-nm light (30 min) then measured with 266-nm light (corresponding curves marked in Figs. 5 and 6). It can be easily seen that the 2.8-eV PL band becomes enhanced with respect to the green and red bands when much power 193-nm light is applied for the 15-nm silica nanoparticles (compare curves 2 and 3 in Fig. 5). In contrast, the same increase in the laser light intensity does not affect the 2.8-eV band efficiency in the 7-nm nanoparticles for the initial and the heat pretreated at $T_{ht}=873$-K samples, whereas the powering of light slightly decreases it in the heat pretreated at $T_{ht}=1173$-K sample (curves 2 and 3 in Fig. 6). Additionally, one can observe a significant enhancement of the 1.9-eV band efficiency for the initial and the heat pretreated at $T_{ht}=873$-K samples of 7-nm particles with powering 193-nm laser light. Meanwhile, the effect becomes small in the case of the heat pretreated at $T_{ht}=1173$-K sample (compare curves 2 and 3 in Fig. 6). At the same time, the intensity of 1.9-eV band measured with 266-nm excitation after preirradiation with strong 193-nm light remains the same for all samples heat pretreated at different temperatures (curve 4 in Fig. 6). If the sample of 15-nm particles heat pretreated at $T_{ht}=873$ K has been preirradiated with 193-nm light, the 1.9-eV band efficiency measured with 266-nm excitation decreases, whereas does not vary for the initial and the heat pretreated at $T_{ht}=1173$-K samples (compare curves 1 and 4 in Fig. 5). As we see, the PL data is very rich reflecting complicated processes occurring in silica nanoparticles. However, before proceeding to a detailed analysis of spectroscopic findings presented in Figs. 5 and 6, let us consider the IDPLY measurements, supporting the conclusion made about the two mechanisms of PL excitation and throwing light on the complicated dynamics of PL spectra presented in the current section.

C. The intensity dependencies of the PL yields (IDPLY)

Figures 7 and 8 show the corresponding IDPLY for discussed PL bands. It is known that the *n*-photon excitation rate (*n* denotes the number of photons that is necessary in order to reach the PL excitation) can be presented as follows: $W^{(n)}=\sigma^{(n)}I_L^n$, where $\sigma^{(n)}$ is the cross section of *n*-photon process and I_L is the laser light intensity.[46] Because the PL intensity is proportional to the MP excitation rate, such power-law dependencies are typical for the MP-excited PL.[11,31,47–49] The usual way to analyze the IDPLY is to draw them in the log-log scale. Then the resulting slope will show the photonicity of the excitation process (Figs. 7 and 8). Accordingly, the IDPLY obtained with 266-nm light is linear, indicating a one-photon process of the PL excitation. As this takes place, the heat pretreatment temperature does not affect the IDPLY slopes. The situation is considerably different with 193-nm excitation. The excitation dynamics is much complicated in this case and includes the saturation conditions. As a result, there are several inflection points, after which the slope changes. The IDPLY-slope for the larger sized particles (15 nm) measured within quite low laser light intensity is $n=1$ for the initial and the heat pretreated at $T_{ht}=873$-K specimens, but it becomes $n=2$ with

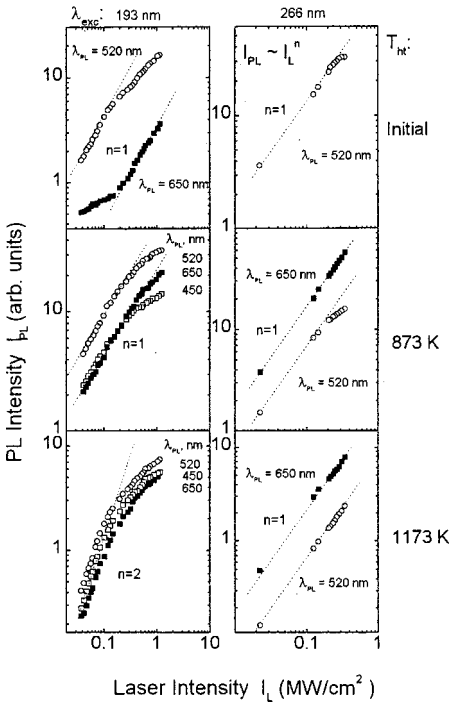

FIG. 7. IDPLY for the 15-nm silica particles heat pretreated at different temperature (T_{ht}) and measured with 193- and 266-nm laser light. λ_{PL} denotes the peak wavelength in the PL spectrum, at which the corresponding IDPLY has been measured. Dashed lines are drawn as a guide to the eye showing different indices for a power function $I_{PL}\sim I_L^n$ in a log-log scale.

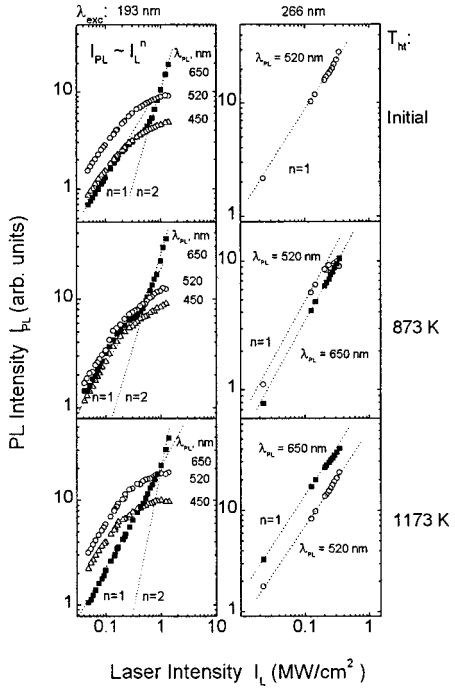

FIG. 8. IDPLY for the 7-nm silica particles heat pretreated at different temperature (T_{ht}) and measured with 193- and 266-nm laser light. λ_{PL} denotes the peak wavelength in the PL spectrum, at which the corresponding IDPLY has been measured. Dashed lines are drawn as a guide to the eye showing different indices for a power function $I_{PL}\sim I_L^n$ in a log-log scale.

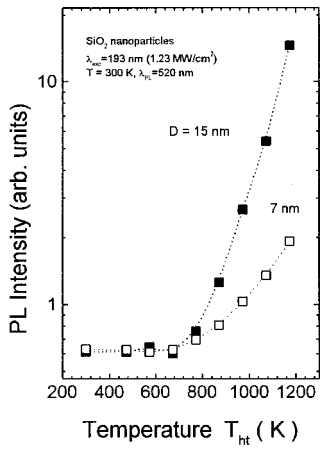

FIG. 9. The heat pretreatment temperature dependencies of the 2.37-eV PL band intensity for the 15- and 7-nm silica nanoparticles in semilogarithmic scale. $\lambda_{exc}=193$ nm, $I_L=1.23$ MW/cm^2.

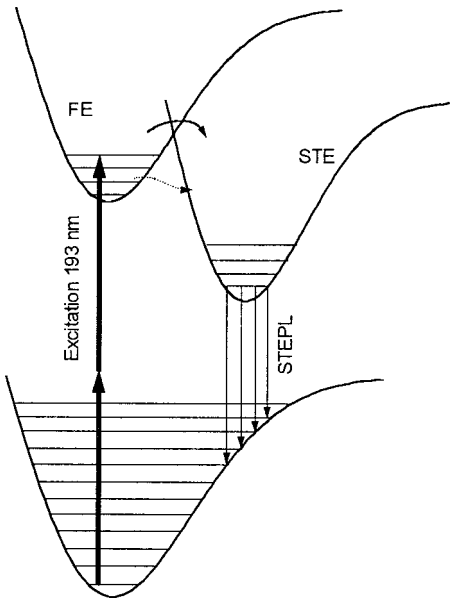

FIG. 10. Schematic diagram in the terms of chemical bonding in ≡Si-O-Si≡ clusters for the self-trapping process of FE's in silica and corresponding absorption and emission transitions. The solid and dashed arrows show the two possibilities for the barrier penetration by activation or by tunneling, respectively.

increasing heat pretreatment temperature to $T_{ht}=1173$ K (Fig. 7). As a finale stage, which can be reached at stronger light, there is an inflection point and the slope changes, normally approaching to the value, which is less than that for the initial stage. The IDPLY slope remains close to linear for all samples heat pretreated at different temperatures and measured within relatively low laser light intensities in the case of 7-nm particles, but it increases up to $n=2$ for the 1.9-eV band when the PL yield becomes saturated (Fig. 8).

Careful analysis of IDPLY slopes allows one to confirm the conclusion made in the preceding section that the mechanism of PL excitation with 266- and 193-nm laser light is completely different. Since the FE dynamics is assumed to be strongly dependent on the nanoparticle surface condition, the IDPLY slope variation in the case of 193-nm light with heat pretreatment temperature is suggested to reflect the peculiarities of the FE energy relaxation in the confined space of silica nanoparticles. For instance, as we mentioned above, the FE relaxation on the surface NBOHC's occurs without energy transfer (an elastic scattering). Therefore, if the concentration of surface NBOHC's increases with increasing heat pretreatment temperature (see Sec. 3.1), the FE density in silica nanoparticles dehydrated at $T_{ht}>873$ K should be much higher than that in untreated samples.

Some additional fact supporting the influence of the surface condition on the FE dynamics is a significant increase in the PL intensity as a whole with increasing heat pretreatment temperature. It can be easily seen from Fig. 9 that the PL intensity increases dramatically within the same temperature range where the free hydroxyl groups transform into NBOHC's (compare Figs. 3 and 9). Therefore, if hydroxyl groups cover the nanoparticle surface, we predict the FE quenching by the surface ≡Si-OH group, probably with hydrogen releasing. As a result, the FE density in the nanoparticle remains quite low and the FE energy transfer to PL centers is inefficient. Accordingly, the quantum efficiency of PL at the mentioned situation is low. However, after heat pretreatment at temperature over $T_{ht}=873$ K the free hydroxyls becomes replaced by NBOHC's(≡Si-O•). Because of the elastic scattering of FE's by the surface NBOHC's one can reach a high density of FE's in the nanoparticle. The energy transfer to PL centers in this case is dominant, resulting in the extremely high efficiency of emission. Note that the 2.8-eV PL band related to STE's also enhances, much as the bands related to the hydrogen impurity and structural defects. We explain this fact as resulting from an increase in the concentration of STE's in nanoparticle. It is evident that the energy transfer through FE's occurs when the FE mean kinetic energy is less than the activation barrier for self-trapping (Fig. 10). However, there is some probability of the STE barrier penetration by tunneling.[44] Since the mentioned probability does not depend on the FE density in the nanoparticle, the STE concentration is proportional to the FE density. This is a reason why all the PL bands discussed grow in intensity simultaneously. On the other hand, there is nothing of the kind in the case of 266-nm laser light, indicating the ordinary one-photon excitation of intrinsic PL from NBOHC's and hydrogen-related centers.

From our point of view, an increase in the concentration of surface NBOHC's with T_{ht} affects the IDPLY measured with 193-nm excitation as well. As we mentioned above, the IDPLY slopes reflect the photonicity of the excitation processes. It should be noted that this statement is true only for intrinsic transitions in isolated PL centers and in the case of direct electron-hole recombination in solid state. Therefore, the value $n=1$ for IDPLY measured with 266-nm excitation really corresponds to a one-photon process. However, this is not the case if the FE energy transfer is involved into the total process of PL excitation. The resulting IDPLY slopes could be less than $n=2$, despite the fact that the excitation results from a TP absorption process. This happens because several radiationless channels occur in the FE energy relaxation in the nanoparticle and on its boundary, but the PL efficiency measured is determined exclusively by a rate of the radiationless energy transfer to light-emitting centers. Since the IDPLY slope variation with T_{ht} is similar for all PL bands discussed (Figs. 7 and 8), we propose that the FE

quenching by the boundary more strongly affects the FE density in silica nanoparticles than the FE energy transfer to PL centers and self-trapping. It should be noted that the laser light intensity dependency of the spin density of defects induced by 193-nm light in the bulk silica reveals the slope $n=2$, indicating a TP process.[2] This fact additionally supports our statement about a dominant role of the nanoparticle boundary in the FE dynamics. So, if the FE quenching by the boundary of 15-nm particles is dominant (the initial sample), then the resulting IDPLY slope is less than $n=2$, whereas the situation approaches to the bulk silica when an elastic scattering of FE's by the nanoparticle boundary takes place ($T_{ht}=1173$ K). From this we conclude that the IDPLY slope tends to be less than $n=2$ when there exists some effective channel in the FE density reduction. One can predict that not only the FE quenching by the nanoparticle boundary reduces the IDPLY slope, but the high rate of the FE self-trapping will reduce it as well. The mentioned situation is suggested to occur for 7-nm particles. As we will show in the next section, because the laser heating effect increases the FE mean kinetic energy in 7-nm particles more effectively than that for 15-nm ones, it becomes large enough, so it exceeds the STE barrier. As a result, the FE self-trapping becomes dominant and reduces the FE density. We consider this feature as a reason why the IDPLY slope measured within quite small laser light intensities for 7-nm silica particles is less than $n=2$ (Fig. 8). In general, one can conclude that if an indirect process of the PL excitation in the silica nanoparticle takes place, the resulting IDPLY slope does not reflect directly the photonicity of the absorption process, because of several pathways in the FE energy relaxation.

One of the most important facts afforded from IDPLY measurements is associated with the saturation condition occurring for 7-nm silica nanoparticles, after which the IDPLY slope for the 1.9-eV band becomes $n=2$ (Fig. 8). Note that this feature is observed only for the band related to the bulk NBOHC's and can be attributed to the formation of Frenkel defect with their subsequent transformation into NBOHC's [reaction (1)]. As a result, the concentration of bulk NBOHC's increases with respect to that thermally produced by heat pretreatment (see Sec. 3.1). Since the indirect PL excitation through the TP-produced FE's involves both of the defect kinds produced by temperature and by irradiation, the 1.9-eV PL band rises up with laser light intensity quadratically. The mentioned fact indicates that the defect generation process is possible only when the laser light intensity is in excess of some critical value, after which the saturation of TP absorption in silica nanoparticles occurs, likely to reflect the FE density saturation. We propose that the FE density at this condition becomes high enough so the biexcitons can be formed. It is natural to assume that the formation of the biexciton immediately leads to its self-trapping. It has been shown for the indirect gap semiconductors that the mean kinetic energy per electron-hole pair in the biexciton with respect to the single FE, increases.[50] From this we predict that the resulting FE mean kinetic energy in the biexciton becomes large enough, so exceeds the STE barrier. The further radiationless decay of self-trapped biexcitons leads to the formation of Frenkel defects with their subsequent transformation into NBOHC's. This model is an extension of the model proposed by Tsai and Griscom.[9]

Let us turn now to the nature of the FE density saturation in silica nanoparticles. Because the FE in silicon dioxide is associated with the replacement of oxygen atom in Si-O-Si bond from its equilibrium position,[1,7] the number of FE's which could be produced, depends generally on the number of Si-O-Si bonds in the silica nanoparticle. As a result, the saturation of the FE density can be reached when most of the Si-O-Si bonds are involved in the generation process of FE's and their motion. Thus, we propose that the FE density saturation is caused by the terminal number of Si-O-Si bonds in the silica nanoparticle. It is evident that the possibility of reaching the FE density saturation for the smaller sized silica nanoparticles is very probable. The presence of NBOHC's will also affect the saturation condition. As we mentioned above, the elastic scattering of FE's by the surface NBOHC's is expected to be a reason for the high FE density in the nanoparticle. In contrast, if the surface is covered by hydroxyls, the FE density is low. On the other hand, the formation of each of the bulk structural defects decreases the total number of Si-O-Si bonds where FE's could be produced. Additionally, since there is a FE energy transfer to bulk NBOHC's followed by their excitation and emission, these PL centers can be considered as some of the kinds of trapping centers, which also will effectively reduce the FE density. Finally, we can conclude that the saturation of the FE density is affected by the size of nanoparticles, by the FE quenching on the surface, and by the FE trapping inside nanoparticles and on their surfaces. As a result of this we predict that the extremely high FE density can be reached for smaller sized defectless nanoparticles with the low concentration of the surface hydroxyl groups.

Note two important peculiarities of the FE dynamics for the smaller sized nanoparticles. Firstly, the FE density saturation can be reached even for the initial untreated sample (Fig. 8). As we mentioned above, the FE quenching by the surface hydroxyls is dominant at this surface condition for 15-nm particles. On the other hand, it is known that the concentration of the free hydroxyl groups in 7-nm silica particles is very low, because the surface hydroxyls are usually bounded in waterlike interfacial species, which are PL centers.[39] The mentioned feature is suggested to be a reason for the saturation of FE density even for the initial sample of 7-nm silica nanoparticles. Secondly, the critical intensity discussed above is affected by the concentration of thermally produced bulk NBOHC's. Figure 8 shows that the critical intensity value is shifted towards higher intensities for the heat pretreated at $T_{ht}=1173$-K sample. We explain this fact as resulting from the FE density lowering due to the high concentration of bulk NBOHC's. The FE density saturation in this case can be reached at the higher intensity of laser light than that for defectless nanoparticles. Finally one can conclude that both of kinds of NBOHC's located inside silica nanoparticles and on their surfaces, affect the FE density. However, the FE elastic scattering by the boundary is responsible for an increase in the FE density, whereas the bulk NBOHC's effectively reduces it.

As evidenced by the foregoing, a high-level resistance to 193-nm laser light characterizes the 15-nm particles. The structural defects were not produced in this material even with the laser light intensity at which it usually happens in the bulk silica.[4,18] On the other hand, the PL efficiency for

15-nm nanoparticles is much higher than that for 7-nm ones (Fig. 9). It can be observed visually as the flashes of light with an extremely high brilliancy passing through the whole visible spectral range. The discovered property of 15-nm silica nanoparticles is expected to be very promising for technological applications.

D. An analysis of the PL spectra dynamics

Let us turn now back to Figs. 5 and 6 and analyze PL properties of silica nanoparticles taking into account the FE energy relaxation model presented in the preceding section. As we mentioned in the Sec. B, the intensity of 1.9-eV PL band related to the bulk NBOHC's for 7-nm nanoparticles increases dramatically when the 193-nm laser light intensity becomes higher than that of the critical intensity (Fig. 6, curves 2 and 3). However, such a feature does not appear for the PL response in the case of 15-nm particles, despite the fact that the same laser light intensity was used (Fig. 5). We associate that with the FE density saturation in smaller sized silica nanoparticles. As a result of this the formation of biexcitons relaxing into Frenkel defects and subsequently into bulk NBOHC's occurs. The formation of exclusively bulk NBOHC's is evidenced by an increase in intensity only for the 1.9-eV band. Thus, the irradiation of 7-nm nanoparticles with 193-nm laser light is a compound process involving both a PL excitation through the TP-produced FE's and the NBOHC's formation, normally occurring at stronger laser light. The 193-nm light generated defects in the 7-nm particles are stable in time, and therefore can be easily detected with 266-nm excitation. It can be seen from Fig. 6 (curves 3 and 4) that the red PL band induced by 193- and 266-nm light is comparable in intensity for the initial and the heat pretreated at T_{ht}=873-K samples. On the other hand, the efficiency of the NBOHC generation by 193-nm light remains to be very high for the heat pretreated at T_{ht}=1173-K sample (it can be seen from curves 1 and 4 in Fig. 6), but the PL excitation through the FE's is inefficient (Fig. 6, curve 3). We explain this feature as being caused by the high concentration of thermally produced bulk NBOHC's. Since the total number of Si-O-Si bonds where FE could be produced is small in this case, the efficiency of the FE energy transfer to the bulk NBOHC's should be very low.

In contrast, the FE density saturation for the 15-nm particles was not achieved even for the heat pretreated at T_{ht}=1173-K sample, as we mentioned above. Accordingly, some additional concentration of bulk NBOHC's cannot be produced in this sample and the intensity of red PL induced by 266-nm light, both before and after preirradiation with 193-nm light, coincide very closely (Fig. 5). However, the red PL band becomes a little weaker for the 15-nm particles heat pretreated at T_{ht}=873 K, which were preirradiated by 193-nm light (Fig. 5). The preirradiation affects only surface NBOHC's, because the resulting red PL peak simultaneously decreases and approaches to the position corresponding to the bulk NBOHC's (1.9 eV) (Fig. 5, curves 1 and 4). From our point of view, the specific feature discussed results from a decrease in the concentration of thermally produced surface NBOHC's due to 193-nm irradiation. We have proposed above that the FE collision with the surface NBOHC occurs without energy transfer as an elastic scattering. Now we improve the model by the fact that such a picture does not always happen with FE's. The mentioned elastic scattering of FE's by the surface NBOHC's takes place only at the situation when the surface of silica nanoparticles is dominantly covered by NBOHC's (T_{ht}=1173 K). If this is not the case (T_{ht}=873 K), the process is expected to be either as an elastic scattering or quenching. We assume that the last process could involve probably the oxygen desorption. All peculiarities discussed for the FE energy relaxation on the nanoparticle boundary are not completely clear and call for further experimental and theoretical studies.

Now let us discuss the dynamics of the blue PL band assigned to STE's. This band is absent for the initial sample of the larger sized particles (Fig. 5). Despite this fact, the maximum of the PL intensity can be achieved at T_{ht} =873 K, whereas the intensity becomes lower for the heat pretreated at T_{ht}=1173-K sample. The mentioned features reflect the strong effect of the silica nanoparticle surface condition on the self-trapping process. As we noted in the preceding section, the FE energy transfer occurs when the FE mean kinetic energy is not enough to pass over the STE potential barrier (Fig. 10). However, this statement can be violated in the case of the heated FE's. We propose that the hot FE's can be produced within the TP process of their generation. The main specific feature of this process is the fact that the FE's are generated on the condition that an intense laser light is applied. It is known that the probability of TP transitions is usually low,[46] so it requires that much power light to be used than that for one-photon excitation. Additionally, the mean-free path length for the FE's(L) in the bulk silicas is much longer than the nanoparticle diameter. For instance, for type-III fused silica, which is a hydrogen-contained material, so it is very close in properties to amorphous silica nanoparticles measured, $L \sim 500$ nm.[1] The last feature allowed us to suggest that the FE's should suffer collisions with the nanoparticle boundary. As we mentioned above, the FE is able to either disappear nonradiatively on the boundary or being elastically scattered, depending on the kind of surface species, with which the FE interacts. At the mentioned condition the FE's can additionally gain energy from a laser field and be heated up to high temperature. Of course, when the FE mean kinetic energy is more than what is necessary for the self-trapping activation, the efficiency of self-trapping increases dramatically, appearing as an increase in the PL intensity related to the STE's (Fig. 10). Figure 5 shows an increase in the STEPL band for the 15-nm particles with increasing laser light intensity, which we attribute to the laser heating of FE's (compare curves 2 and 3 in Fig. 5). Since the probability of the FE quenching by the boundary for the initial sample is very high (see Sec. 3.3), the efficiency of the laser heating of FE's is low. As a result, the rate of the FE penetration through the STE barrier will be also low. Hence, the self-trapping of FE's is inefficient and the corresponding STEPL band appears itself with small intensity. The efficiency of the laser heating becomes much higher for the heat pretreated at T_{ht}=873-K sample, because of the elastic scattering of FE's on the nanoparticle boundary. Accordingly, the intensity of the STEPL band increases. Because of an increase in the concentration of thermally produced bulk NBOHC's for the heat pretreated at T_{ht}=1173-K sample, the FE density be-

comes lower and the STEPL intensity decreases, whereas the laser heating rate remains high (curves 2 and 3 in Fig. 5). Hence, the model of FE energy relaxation presented in the Sec. C quite reasonably explains all above-mentioned features for STEPL band in the 15-nm silica nanoparticles.

The STEPL band for the smaller sized nanoparticles appears for all samples heat pretreated at different temperatures. Moreover, the intensity of the PL bands for the initial and the heat pretreated at T_{ht}=873-K samples does not vary with the 193-nm light intensity, but slightly decreases for the heat pretreated at T_{ht}=1173-K sample (curves 2 and 3 in Fig. 6). According to the above-presented model of the FF energy relaxation in silica nanoparticles, one can assume that the FE's are heated up to the energy exceeding the STE barrier in 7-nm particles even at weak 193-nm light used. Because of the low concentration of free hydroxyl groups on the 7-nm nanoparticle surface, the FE's can be elastically scattered from the nanoparticle boundary gaining some additional energy from a laser field. We predict that the FE's suffer many collisions, increasing their mean kinetic energy after each collision (the laser heating process). It is evident that the frequency of collisions in the nanoparticle tends to be higher with decreasing diameter. Hence, the efficiency of FE laser heating is expected to be higher in the smaller sized nanoparticles. From this point of view, the FE density saturation discussed in the preceding section should be retermed in a more correct form as a saturation of the hot FE density. The high rate of the FE laser heating is a reason why the STEPL band can be observed for the initial sample of 7-nm particles compared to that of 15-nm ones. The further gain in the FE energy with increase in the laser light intensity does not affect more the efficiency of the STE barrier penetration in this case. As a result, the STEPL band intensity does not vary with laser light intensity for the initial and the heat pretreated at T_{ht}=873-K samples. A fall in the PL efficiency with increasing laser light intensity for the heat pretreated at T_{ht}=1173-K sample can be attributed to a FE density reduction due to the high concentration of thermally produced bulk NBOHC's.

Note that the mentioned FE laser heating process is similar to that of the electron laser heating in a ionized plasma[51–53] and under the MP ionization of molecular ions adsorbed on the silica nanoparticle surface.[35,54] We propose that this process is a specific feature of TP-produced FE's in silica nanoparticles, and it should be taken into account in studies of the FE dynamics in the wide band-gap nanoscale objects.

As we see, the dynamics of TP-produced FE's in silica nanoparticles is very complicated and calls for a separate theoretical study. The correct description of these dynamics requires to take into account the TP absorption process in the FE generation, the quenching and elastic scattering by the nanoparticle boundary, the energy transfer to impurities and structural defects, and the biexciton model for the Frenkel defect formation.

IV. CONCLUSIONS

The experimental results presented in the current paper unambiguously show that the PL from silica nanoparticles induced by 6.4-eV ArF laser light is associated with the relaxation of TP-produced FE's.

It has been established that the PL results from the STE's as well as from the surface hydrogen-related centers and bulk NBOHC's excited through the radiationless relaxation of FE's.

We propose that there exists some activation barrier for FE's to be self-trapped, which can be overcame with increase in the FE mean kinetic energy owing to the laser heating. The last process is assumed to be due to elastic collisions with the nanoparticle boundary on the condition that a strong laser field is used as required of TP excitation.

It has been shown that the nanoparticle surface condition strongly affects the FE dynamics, including the laser heating of FE's with subsequent self-trapping, the energy transfer to hydrogen-related centers and NBOHC's, and the Frenkel defect formation.

We have found the high-level resistance to 193-nm laser light for 15-nm silica nanoparticles. The structural defects were not produced in the material with laser light intensity, at which in the bulk silica the efficiency usually is quite high. The mentioned resistance becomes lower for 7-nm silica nanoparticles appearing in the formation of NBOHC's.

One can reach the high density of FE's in the dehydrated 15-nm silica nanoparticles resulting in an extremely high PL efficiency. The discovered property for the 15-nm silica nanoparticles is expected to find numerous applications in nanoscale technology and quantum electronics.

ACKNOWLEDGMENTS

The authors acknowledge Academia Sinica, National Science Council (Contract No. 89-2113-M-001-032), and the China Petroleum Corporation of Taiwan, Republic of China, for financial support.

*Corresponding author: E-mail: glinka@po.iams.sinica.edu.tw

[1] A. N. Trukhin, J. Non-Cryst. Solids **149**, 32 (1992).
[2] K. Arai, H. Imai, H. Hosono, Y. Abe, and H. Imagawa, Appl. Phys. Lett. **53**, 1891 (1988).
[3] C. Itoh, K. Tanimura, N. Itoh, and M. Itoh, Phys. Rev. B **39**, 11 183 (1989).
[4] K. Awazu and H. Kawazoe, J. Appl. Phys. **68**, 3584 (1990).
[5] H. Nishikawa, R. Nakamura, R. Tohmon, Y. Ohki, Y. Sakurai, K. Nagasawa, and Y. Hama, Phys. Rev. B **41**, 7828 (1990).
[6] C. Itoh, T. Suzuki, and N. Itoh, Phys. Rev. B **41**, 3794 (1990).
[7] A. Shluger and E. Stefanovich, Phys. Rev. B **42**, 9664 (1990).
[8] H. Imai, K. Arai, H. Hosono, Y. Abe, T. Arai, and H. Imagawa, Phys. Rev. B **44**, 4812 (1991).
[9] T. E. Tsai and D. L. Griscom, Phys. Rev. Lett. **67**, 2517 (1991).
[10] D. L. Griscom, J. Ceram. Soc. Jpn. **99**, 923 (1991).
[11] W. Joosen, S. Guizard, P. Martin, G. Petite, P. Agostini, A. Dos Santos, G. Grillon, D. Hulin, A. Migus, and A. Antonetti, Appl. Phys. Lett. **61**, 2260 (1992).
[12] N. Kuzuu, Y. Matsumoto, and M. Murahara, Phys. Rev. B **48**, 6952 (1993).
[13] L. Skuja, J. Non-Cryst. Solids **179**, 51 (1994).
[14] M. Wilson, P. A. Madden, M. Hemmati, and C. A. Angell, Phys. Rev. Lett. **77**, 4023 (1996).
[15] L. Skuja and B. Guttler, Phys. Rev. Lett. **77**, 2093 (1996).

[16] L. Skuja, K. Tanimura, and N. Itoh, J. Appl. Phys. **80**, 3518 (1996).
[17] A. Pasquarello and R. Car, Phys. Rev. Lett. **79**, 1766 (1997).
[18] N. Kuzuu, T. Taga, and N. Kamisugi, J. Appl. Phys. **81**, 8011 (1997).
[19] B. Guillot and Y. Guissani, Phys. Rev. Lett. **78**, 2401 (1997).
[20] M. Boero, A. Pasquarello, J. Sarnthein, and R. Car, Phys. Rev. Lett. **78**, 887 (1997).
[21] N. Nishikawa, Y. Miyake, E. Watanabe, D. Ito, K. S. Seol, Y. Ohki, K. Ishii, Y. Sakurai, and K. Nagasawa, J. Non-Cryst. Solids **222**, 221 (1997).
[22] G. Pacchioni, G. Ierano, and A. Marquez, Phys. Rev. Lett. **81**, 377 (1998).
[23] L. Skuja, J. Non-Cryst. Solids **239**, 16 (1998).
[24] L. Skuja, B. Guttler, D. Schiel, and A. R. Silin, Phys. Rev. B **58**, 14 296 (1998).
[25] M. A. Stevens Kalceff, Phys. Rev. B **57**, 5674 (1998).
[26] G. Pacchioni and M. Vitiello, Phys. Rev. B **58**, 7745 (1998).
[27] H. Hosono, H. Kawazoe, and N. Matsunami, Phys. Rev. Lett. **80**, 317 (1998).
[28] D. L. Griscom and M. Mizuguchi, J. Non-Cryst. Solids **239**, 66 (1998).
[29] D. L. Griscom, *in Proceedings of the Thirty-Third Frequency Control Symposium* (Electronics Industries Association, Washington, D.C., 1979), p. 98.
[30] G. Lucovsky, J. Yang, S. S. Chao, J. E. Tyler, and W. Czubatyj, Phys. Rev. B **28**, 3225 (1983).
[31] Yu. D. Glinka, S. N. Naumenko, and V. Ya. Degoda, J. Non-Cryst. Solids **152**, 219 (1993).
[32] M. S. El-Shall, S. Li, T. Turkki, D. Graiver, U. C. Pernisz, and M. I. Baraton, J. Phys. Chem. B **99**, 17 805 (1995).
[33] K. S. Seol, Y. Ohki, H. Nishikawa, M. Takiyama, and Y. Hama, J. Appl. Phys. **80**, 6444 (1996).
[34] Yu. D. Glinka and M. Jaroniec, J. Appl. Phys. **82**, 3499 (1997).
[35] Yu. D. Glinka, Zh. Eksp. Teor. Fiz **111**, 1748 (1997) [JETP **84**, 957 (1997)].
[36] M. Goldberg, H.-J. Fitting, and A. Trukhin, J. Non-Cryst. Solids **220**, 69 (1997).
[37] A. N. Trukhin, M. Goldberg, J. Jansons, H.-J. Fitting, and I. A. Tale, J. Non-Cryst. Solids **223**, 114 (1998).
[38] S. M. Prokes, W. E. Carlos, S. Veprek, and Ch. Ossadnic, Phys. Rev. B **58**, 15 632 (1998).
[39] Yu. D. Glinka, S. H. Lin, and Y.-T. Chen, Appl. Phys. Lett. **75**, 778 (1999).
[40] L. E. Brus, P. F. Szajowski, W. L. Wilson, T. D. Harris, S. Schuppler, and P. H. Citrin, J. Am. Chem. Soc. **117**, 2915 (1995).
[41] D. W. Cooke, B. L. Bennett, E. H. Farnum, W. L. Hults, K. E. Sickafus, J. F. Smith, T. N. Taylor, and P. Tiwari, Appl. Phys. Lett. **68**, 1663 (1996).
[42] M. Zhu, Y. Han, R. B. Wehrspohn, C. Godet, R. Etemadi, and D. Ballutaud, J. Appl. Phys. **83**, 5386 (1998).
[43] J. Yuan, D. Haneman, I. Andrienko, and W. Li, J. Appl. Phys. **83**, 4385 (1998).
[44] E. I. Rashba, *in Excitons; Selected Chapters*, edited by E. I. Rashba and M. D. Sturge (Elsevier, Amsterdam, 1987), p. 273.
[45] Yu. D. Glinka, T. B. Krak, Yu. N. Belyak, V. Ya. Degoda, and V. M. Ogenko, J. Colloids Surf. A **104**, 17 (1995).
[46] Y. R. Shen, *The Principles of Nonlinear Optics* (Wiley, New York, 1984).
[47] Yu. D. Glinka, Appl. Phys. Lett. **70**, 1336 (1997).
[48] Yu. D. Glinka, K.-W. Lin, H.-C. Chang, and S. H. Lin, J. Phys. Chem. B **103**, 4251 (1999).
[49] R. P. Chin, Y. R. Shen, and V. Petrova-Koch, Science **270**, 776 (1995).
[50] V. B. Timofeev, *in Excitons; Selected Chapters*, edited by E. I. Rashba and M. D. Sturge (Elsevier, Amsterdam, 1987), p. 229.
[51] F. B. Bunkin, A. E. Kazakov, and M. V. Fedorov, Usp. Fiz. Nauk **109**, 117 (1973) [Sov. Phys. Usp. **16**, 416 (1973)].
[52] N. M. Kroll and K. M. Watson, Phys. Rev. A **8**, 804 (1973).
[53] N. I. Koroteev and I. L. Shumay, *Physics of High-Power Laser Radiation* (Nauka, Moscow, 1991) (in Russian).
[54] Yu. D. Glinka and M. Jaroniec, Phys. Rev. A **56**, 3056 (1997).